Journal Pre-proofs

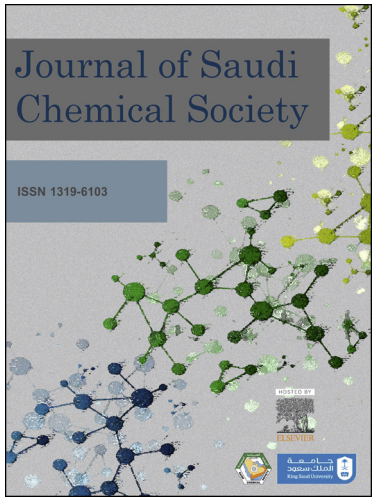

Original article

Selective Catalytic Transformation of Polystyrene into Ethylbenzene over Fe-Cu-Co/Alumina

Nouf M. Aljabri, Zhiping Lai, Kuo-Wei Huang

PII: S1319-6103(20)30008-9
DOI: https://doi.org/10.1016/j.jscs.2020.01.008
Reference: JSCS 1104

To appear in: *Journal of Saudi Chemical Society*

Received Date: 31 August 2019
Revised Date: 16 January 2020
Accepted Date: 19 January 2020

Please cite this article as: N.M. Aljabri, Z. Lai, K-W. Huang, Selective Catalytic Transformation of Polystyrene into Ethylbenzene over Fe-Cu-Co/Alumina, *Journal of Saudi Chemical Society* (2020), doi: https://doi.org/10.1016/j.jscs.2020.01.008

Selective Catalytic Transformation of Polystyrene into Ethylbenzene over Fe-Cu-Co/Alumina

Nouf M. Aljabri,[a,b] Zhiping Lai,[a,c] and Kuo-Wei Huang [a,b,*]

[a]Division of Physical Science and Engineering, King Abdullah University of Science and Technology, Thuwal 23955-6900, Saudi Arabia.

[b]KAUST Catalysis Centre, King Abdullah University of Science and Technology, Thuwal 23955-6900, Saudi Arabia.

[c]Advanced Membranes & Porous Materials Centre, King Abdullah University of Science and Technology, Thuwal 23955-6900, Saudi Arabia.

hkw@kaust.edu.sa

Abstract

FeCuCo over aluminum oxide catalyst was prepared to catalytically degrade polystyrene (PS) into ethylbenzene (EB) under mild conditions. This catalyst was characterized by XRD, SEM, STEM-EELS, STEM-EDS, XPS, and physical properties. A significant selectivity toward EB formation at 250 °C was achieved in the absence of hydrogen with 82% liquid yield. End-chain session and cross-linking reactions are proposed to be the dominant pathways in the degradation of PS over FeCuCo to form EB.

Keywords: (Polystyrene, catalytic-degradation, Ethylbenzene, selective-conversion)

1. Introduction

The production of plastic was increased by twenty times in the last fifty years because of the continuous increase in human activities [1]. In 2015, plastic production in the packaging sector had achieved 40% of the total plastic production due to their several advantages [1]. The global plastic packaging sector share was increased from 17 to 25% in the period from 2000-2015 due to the high market need [2]. However, about 95% of these plastic products are disposed of after a single-use, not only causing a severe waste management issue, but an annual economic loss estimated to be $80-120 billion [2].

Polystyrene (PS) is one of the foremost polymers in the packaging sector due to its inexpensive cost as well as many preferred properties. Its production has reached $15 million by 2008 [3]. Notwithstanding with PS high demand and production rate, PS is well-known for its reduced recycling rate making the landfill is the primary route worldwide to handle its waste [4]. Kwon et al. have investigated the presence of styrene monomers, dimers and trimers in samples of beach sands and seawater from different regions. Notably, all the samples showed a high content of styrene analogues [5].

Indeed, developing energy-efficient catalysts to convert PS into valuable chemicals can improve the plastic economy and relief PS pollution. The bi and tri-metallic catalysts' performance can surpass their mono-counterparts because of the synergy between the existed metallic-sites. Fe-Cu/Alumina was used to catalyze the conversion of PS quantitatively into aromatics such styrene monomer with 66% liquid yield at 250 °C in batch conditions [6]. The use of Fe-Co/Alumina has substantially increased the liquid yield from 66% to 91%, where the styrene recovery was boosted-up to reach 45 wt.% at 250 °C [7]. However, the recycled-styrene polymerization leads to synthesize low-quality polymers with reduced average molecular weight and low glass transition temperature, which limits their application. The primary reason for this low-quality is the presence of polycyclic aromatic hydrocarbons (PAH) impurities in

the recovered styrene yield, which act as chain transfer agents [8]. Therefore, catalytically converting PS into valuable chemicals other than styrene that can be used as precursors to synthesize a wide range of products is highly needed.

Herein, we report a catalyst system that degrades PS selectively into EB instead of styrene. EB is a stable compound during the storage and can be converted into styrene monomer as needed. EB can also be employed as an anti-knock agent to gasoline, as a solvent for pesticides, cellulose acetate, paints, inks and synthetic rubbers, and as the starting material for acetophenone, diethyl benzene, and ethyl-anthraquinone. Our Fe-Cu-Co/ Al_2O_3 showed a remarkable 82% liquid yield with 82% selectivity towards EB at 250 °C for 90 minutes at the full conversion of PS.

2. Experimental details

2.1. Materials

Alumina (Al_2O_3), iron (III) nitrate nonahydrate $Fe(NO_3)_3.9H_2O$, cupric nitrate trihydrate $Cu(NO_3)_2$ $3H_2O$, cobalt nitrate hexahydrate $Co(NO_3)_2 \cdot 6H_2O$. Bimodal PS tablets with an average molecular weight (Mw) of 96,000 g/mol were purchased from Sigma-Aldrich and used without further treatment. All PS samples were crushed to achieve an average particle size of 100 μm before the degradation reaction to enhance the contact with the catalyst. All solvents used for gas chromatography /mass spectrometry (GC/MS, Agilent) and gel permeation chromatography (GPC) calibration were (HPLC grade) and purchased from Sigma-Aldrich.

2.2. Fe-Cu-Co/Alumina synthesis

Fe-Cu-Co/Al_2O_3 was synthesized by the co-impregnation method. ɣ-alumina (15.0 g) was incubated in a vacuum oven for three hours at 110 °C to remove moisture and any impurities from alumina pores. The impregnation solution was prepared by dissolving iron (III) nitrate nonahydrate (1.50 g), cobalt nitrate hexahydrate (1.0 g) and cupric nitrate trihydrate (0.50 g) in 10.0 mL deionized water. Later, the impregnation solution was added to 5.0 g of ɣ-alumina

in which is slightly higher than the pores volume. Then, the slurry was stirred at 60 °C for three hours, dried in a vacuum oven for overnight at 110 °C. Finally, the Fe-Cu-Co/Al_2O_3 was calcined at 550 °C for four hours in an oxidative environment.

2.3. Fe-Cu-Co/Alumina characterization

BET surface areas of Fe-Cu-Co/Alumina and blank alumina were measured by surface area and porosity analyzer ASAP2420 Micrometrics using nitrogen adsorption and desorption at 77.4 K. The metal oxides distribution among the alumina surface was indicated by transition electron microscopy (TEM)/ electron energy loss spectroscopy (EELS) and the Energy-dispersive X-ray spectroscopy (EDS). The surface morphology of the impregnated catalyst before and after the reaction was determined by scanning electron microscopy (SEM). The temperature-programmed desorption (TPD) measurements were performed on AMI-300 TPD instrument using two probes, NH_3 and CO_2, respectively. Briefly, 0.20 g of each sample was weighed once at a time, and the physisorbed water was removed by preheating the samples at 250 °C in a helium flow for two hours. The reactor was then allowed to cool down to room temperature followed by introducing ammonia into the reactor at 100 °C. After an hour, the physisorbed ammonia was removed under the helium flow at 100 °C. After 30 minutes, the samples were heated from 100 to 800 °C at a heating rate of 10 °C/min. The temperature was fixed for 30 minutes. An on-line gas chromatograph with a TCD detector was used to analyze the effluent gases. For the CO_2-TPD, the same condition was used. The XPS experiments were performed using a Kratos Axis Ultra DLD instrument equipped with a monochromatic Al Kα x-ray source (hν = 1486.6 eV) operated at a power of 150 W and under UHV conditions in the range of ~ 10−9 mbar. All spectra were recorded in hybrid mode using electrostatic and magnetic lenses and an aperture slot of 300 μm × 700 μm. The survey and high-resolution spectra were acquired at fixed analyzer pass energies of 160 eV and 20 eV, respectively. All

the samples were mounted in a floating mode to avoid the differential charging. Therefore, XPS spectra were acquired using charge neutralization.

2.4. Transformation reaction apparatus and analysis

PS transformation reaction was conducted in a Parr reactor. PS loading was fixed to be 2.0 g while the Fe-Cu-Co/Alumina loading was varied from 100.0 to 500.0 mg. PS tablets were crushed to achieve an average particle size of 100 μm and mixed with a weighted amount of the catalyst in a 25 mL reactor vessel before heating. The reactor was then heated to 250 °C using a clamp heater at a rate of 4 °C/ min, and heated for an additional 30-90 minutes before it was allowed to cool down to room temperature. All the reactions were conducted under air. The stirring speed was fixed at 500 rpm in all the reactions

The resulting liquid products were collected, filtered (ION Chrom Acrodisc membrane 0.45 um), and characterized by GC/MS (Agilent 5975C inert XL EI/CI MSD with Triple-Axis MS Detector) and NMR (Bruker Advance 400). The remaining residue in the reactor was dissolved with toluene (10.0 mL). The mixture was filtered and toluene was removed *in vacuo* from the filtrate to give the oligomer mixtures, which were further dried in the vacuum oven at 50 °C until the weights became constant. The samples were dissolved in D-chloroform NMR analysis as in tetrahydrofuran (0.2 g/mL) for GPC analysis. The recovered catalysts were characterized using STEM, TEM-EDS, TEM-EELS, SEM, and XPS (Fig. S1).

3. Results and discussion

3.1. Fe-Cu-Co/Alumina characterization

XRD diffraction patterns of the ɣ-aluminum oxide before and after the metals loading are shown in Figure S2. There is no significant difference in the support's diffractograms before and after the metals impregnation because of the low metals loading. It also indicates a good dispersion of Fe-Cu-Co metals within the alumina matrix. The diffraction peaks at 19.8°, 32°,

37.1°,39.4°, 45.9°, 61.1° and 66.8° correspond to (111), (220), (331), (222), (400), (511) and (4 4 0) in good agreement with those of γ-Al_2O_3 XRD patterns[9, 10].

After the impregnation of metals into alumina, BET surface area was reduced, indicative of successful metals loading into the alumina matrix (Table S1). However, the alumina pore sizes did not change considerably after the loading, indicating that the alumina pore structures were not significantly altered during the impregnation process (Fig. S3a, Table. S1). Furthermore, the aluminum oxide and Fe-Cu-Co/Alumina nitrogen adsorption-desorption isotherms showed a mesoporous structure and type IV hysteresis (Fig. S3b). The surface area of Fe-Cu-Co/Alumina suggested that the PS degradation might take place first on the external surface, followed by a transformation of the resulted oligomers inside the pores to yield the aromatics. The catalyst acidity and basicity play a crucial role in initiating the degradation reactions and tailor the product selectivity [11]. Madras and Karmore have investigated different Lewis acids such as $AlCl_3$ and $FeCl_3$ and showed that the PS degradation starts with hydride elimination from the benzylic carbon by the Lewis acid site resulting in the molecular weight reduction [12]. CO_2-TPD results have shown a reduction in the alumina basicity strength after the metals impregnation. The sharp basicity peak of alumina at 610 °C was shifted to the medium region of 400 °C (Fig. 1a) [11]. The shift of CO_2 desorption towards lower temperature region indicates that the strength of basicity is weaker for the catalyst. Furthermore, the NH_3-TPD indicated an increase in the acidity after the Fe-Cu-Co impregnation into alumina, presumably because of the Lewis acidity of iron in the system (Fig. 1b). This acidity may play a significant role to facilitate the PS degradation under mild conditions.

3.2. Fe-Cu-Co/Alumina catalytic activity

Catalytic PS degradation was conducted by heating a mixture of 2.0 g of PS and 200 mg of the catalyst at 250 °C for 90 minutes. A liquid yield of approx. 82% was obtained with a surprisingly high selectivity towards EB, based on the NMR and GC/MS analysis (Fig. S4). To

the best of our knowledge, such a unique selectivity has never been reported in the literature, while a number of multi-metallic catalysts were prepared and tested for PS degradation (Table 1). None of the monometallic, Fe/Alumina, Cu/Alumina and Co/Alumina and their bi-metallic showed this high selectivity toward EB formation.

To further confirm the results, the reactions were repeated at least three times to ensure the reproducibility (Table 2). This excellent selectivity towards EB in the absence of hydrogen pressure is exceptionally intriguing. One of the most characteristic pathways during PS degradation is the ß-session which involves the chain-end cation to yield the monomer. Similarly in this work, the selective styrene formation can result from ß-session of PS. However, part of PS in the reaction must serve as the hydrogen pool to allow hydrogenation of styrene to EB under the catalytic condition. Indeed, coke formation was found on the spent catalyst as a result of the deposited carbon from PS (Fig. S5). Notably, GPC data also showed that the PS was converted from bimodal to unimodal after the treatment with Fe-Cu-Co/alumina indicating that the PS undergo a series of unzipping reactions to release the monomers (Fig. S6). It is likely that the secondary/crosslinking reaction contributed most to the transformation of SM into EB.

We have also conducted control experiments by employed styrene and EB as starting materials, respectively, under the same conditions. Notably, EB was found as the major product (60 wt. % overall yield) when styrene was used, while some of the styrene polymerized during the reaction (Fig. 2, Fig. S7) No conversion was observed when EB was used alone. These results suggest that styrene can also serve as the hydrogen source for hydrogenation of styrene to EB and EB is stable in the presence of Fe-Cu-Co/Alumina at 250 °C (Fig. 3).

3.3. Exposure time effect

Different exposure time, 30, 60, and 90 min. were analyzed to identify the optimum exposure time. The SM selectivity drastically decreased from 22 wt.% to 7 wt.% when the exposure time

was increased from 30 min. to 90 min. (Fig. 4). In contrary, EB selectivity was increased from 64 wt.% to 81 wt.% when the reaction time increased from 30 min. to 90 min. (Fig. 4). Worth to mention the further increase in the exposure time to 180 min. did not change the obtained result. Since the highest EB selectivity was achieved at 90 min, this exposure time was selected as optimum exposure time.

3.4. Fe-Cu-Co/Alumina loading effect

PS/catalyst ratio could be an integral element to influence the liquid and/or products selectivity. PS degradation was further tested using different catalyst loadings from 100 to 500 mg per 2.00 g of PS. No significant changes in the liquid yields and the product selectivity were observed when increasing the catalyst beyond 200 mg, suggesting 200 mg is the optimum weight for the complete conversion of PS (Fig.5). The starting material was bimodal PS, which converted into unimodal after the degradation (Fig. S7). The increasing in catalyst weight from 100 to 500 mg resulted in lower molecular weights and sharper oligomers peak.

4. Fresh and spent catalysts characterization

Consistent with the XRD patterns, the SEM images of the fresh catalyst did not show any metal clusters and no EELS map could be generated which indicating the homogeneous distribution of the Fe-Cu-Co in the alumina matrix (Fig. S8 a). The presence of Fe-Cu-Co was confirmed by TEM-EDS signals and XPS (Fig. S9, Table. 3). The elemental analysis indicated that the metallic sites Fe, Cu, Co were decreased from 0.78%, 0.37%, and 0.47% before the reaction to 0.38%, 0.25%, and 0.38% after the reaction, respectively. This decrease is likely due to the metals' slight dissolution during the reaction course, although the limitations of EDX and inhomogeniety cannot be ruled out. It should be noted that the compositions of the metals on the catalyst surface identified by XPS is not necessarily the same as the those of the bulk catalyst, especially in the case of the increased sample heterogeneity after the reaction. The decreases in the metal compositions of the spent catalyst may be attributed to the presence of

the deposited carbon on the catalyst's surface after the reaction, which increased the surface complexity of the sample. In contrast to the homogeneity of fresh Fe-Cu-Co/alumina, there are significant metal clusters in the spent catalyst due to the migration of the metals on the deposited carbon and aggregated among themselves (Fig. S8 b) [13, 14]. This accumulated carbon caused an increase in the particle size and reduction in the surface area, and as a result, completely deactivated the catalyst. These observations also indicate that some PS or styrene was fully dehydrogenated.

Carbon elemental analysis showed that the carbon increased from 15.35%, as a baseline, to 38% after the transformation because of the coke formation during the reaction course (Table 3). Furthermore, TEM-ELLS low magnification carbon map showed a shake-up suggesting that the coke source is polymeric where no carbon signal or shake-up feature was indicated in the fresh catalyst. Interestingly, the STEM-EELS images of the spent catalyst showed only copper clusters, confirming a good interaction of Fe-Co with the alumina support. Fe-Cu-Co/Alumina has a nest-like structure morphology that did not change significantly after the reaction (Fig. S10).

5. Conclusion

In summary, PS degradation catalyzed by a Fe-Cu-Co/Alumina catalyst has been demonstrated under mild conditions for the first time to offer a unique selectivity towards EB. Increasing the catalyst loading beyond 200 mg did not alter the products selectivity or liquid yield. EDS has confirmed the presence of the iron, copper and cobalt oxides. The SEM and STEM-EELS did not show any metal clusters in the fresh catalyst, confirming a good metal distribution and interaction with the support. We have presented the first example for selective conversion of PS into EB in a straight forward process and under mild conditions. Further mechanistic investigations are ongoing and will be reported in due course.

Acknowledgement

We are grateful for the generous support from King Abdullah University of Science and Technology (KAUST).

Reference

[1] PlasticsEurope, Plastics – the Facts 2016, Plastics – the Facts 2016, pp. 1-38.
[2] E.M.F.a.M.C. World Economic Forum, The new plastics economy- Rethinking the future of plastics 2016, pp. 1-61.
[3] H.M. Feng, J.C. Zheng, N.Y. Lei, L. Yu, K.H.K. Kong, H.Q. Yu, T.C. Lau, M.H.W. Lam, Photoassisted Fenton Degradation of Polystyrene, Environ Sci Technol, 45 (2011) 744-750.
[4] K. Saido, K. Amamiya, H. Sato, A. Okabe, N. Ogawa, Y. Kamaya, K. Kogure, M. Nishimura, K. Okukawa, T. Kusui, Analysis of Styrene Oligomer Contaminants Generated from Marine Debris Polystyrene on the Coast of Okinawa, BUNSEKI KAGAKU, 61 (2012) 629-636.
[5] B.G. Kwon, K. Saido, K. Koizumi, H. Sato, N. Ogawa, S.Y. Chung, T. Kusui, Y. Kodera, K. Kogure, Regional distribution of styrene analogues generated from polystyrene degradation along the coastlines of the North-East Pacific Ocean and Hawaii, Environ Pollut, 188 (2014) 45-49.
[6] N.M. Aljabri, Z. Lai, N. Hadjichristidis, K.-W. Huang, Renewable aromatics from the degradation of polystyrene under mild conditions, Journal of Saudi Chemical Society, 21 (2017) 983-989.
[7] N.M. Aljabri, Z. Lai, K.-W. Huang, Selective conversion of polystyrene into renewable chemical feedstock under mild conditions, Waste Management, 78 (2018) 871-879.
[8] D.S. Achilias, I. Kanellopoulou, P. Megalokonomos, E. Antonakou, A.A. Lappas, Chemical recycling of polystyrene by pyrolysis: Potential use of the liquid product for the reproduction of polymer, Macromol Mater Eng, 292 (2007) 923-934.
[9] H.F. Jiao, X.L. Zhao, C.X. Lv, Y.J. Wang, D.J. Yang, Z.H. Li, X.D. Yao, Nb_2O_5-gamma-Al_2O_3 nanofibers as heterogeneous catalysts for efficient conversion of glucose to 5-hydroxymethylfurfural, Sci Rep-Uk, 6 (2016).
[10] J.B.A. Lian, J.M. Ma, X.C. Duan, T.I. Kim, H.B. Li, W.J. Zheng, One-step ionothermal synthesis of gamma-Al_2O_3 mesoporous nanoflakes at low temperature, Chem Commun, 46 (2010) 2650-2652.
[11] D.K. Ojha, R. Vinu, Resource recovery via catalytic fast pyrolysis of polystyrene using zeolites, J Anal Appl Pyrol, 113 (2015) 349-359.
[12] V. Karmore, G. Madras, Thermal degradation of polystyrene by Lewis acids in solution, Ind Eng Chem Res, 41 (2002) 657-660.
[13] A.S. Al-Fatesh, M.A. Naeem, W.U. Khan, A.E. Abasaeed, A.H. Fakeeha, Effect of Nano-support and Type of Active Metal on Reforming of CH4 with CO2, J Chin Chem Soc-Taip, 61 (2014) 461-470.
[14] J.A. Moulijn, A.E. van Diepen, F. Kapteijn, Catalyst deactivation: is it predictable? What to do?, Appl Catal a-Gen, 212 (2001) 3-16.
[15] J. Kijenski, T. Kaczorek, Catalytic degradation of polystyrene, Polimery-W, 50 (2005) 60-63.

Figures captions list

Figure 1 Temperature program desorption of Fe-Cu-Co/Alumina and Alumina (a) CO_2 TPD and (b) NH_3 TPD.

Figure 2 PS degradation over Fe-Cu-Co/Alumina (a) the liquid yield versus the remaining oligomers yields (b) products selectivity (Conditions: reaction temperature 250 °C, exposure time: 90 min., catalyst loading: 0.20 g, PS loading: 2.0 g, and under air).

Figure 3 Control experiments of styrene and ethylbenzene reactivity in the presence of Fe-Cu-Co/Alumina (a) product yields and (b) Products selectivity in wt.% (Conditions: reaction temperature 250 °C, catalyst loading: 0.20 g, exposure time: 90 min., and under air).

Figure 4 Exposure time effect on the transformation of PS into EB (Conditions: reaction temperature 250 °C, catalyst weight: 0.20 g, PS weight: 2.0 g, and under air).

Figure 5 Fe-Co-Cu\Alumina loading effect on the products selectivity (Conditions: reaction temperature 250 °C, exposure time: 90 min., PS loading: 2.0 g, and under air).

Tables captions list

Table 1 The reported bimetallic catalysts result in the literature (A* in the table stands for Aromatics).

Table 2 Fe-Cu-Co/Alumina catalytic reproducibility and selectivity (Conditions: reaction temperature: 250 °C, exposure time: 90 min., catalyst weight: 0.20 g)

Table 3 XPS elemental analysis of fresh & spent Fe-Cu-Co/Alumina.

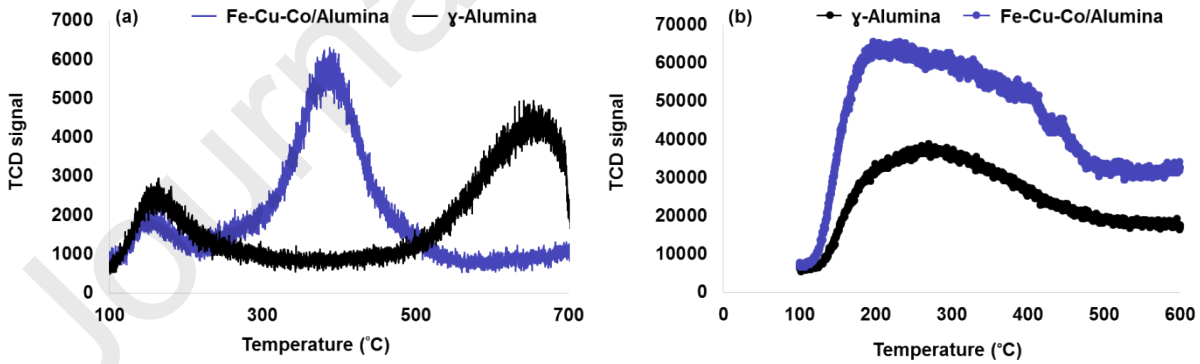

Figure 1 Temperature program desorption of Fe-Cu-Co/Alumina and Alumina (a) CO_2 TPD and (b) NH_3 TPD.

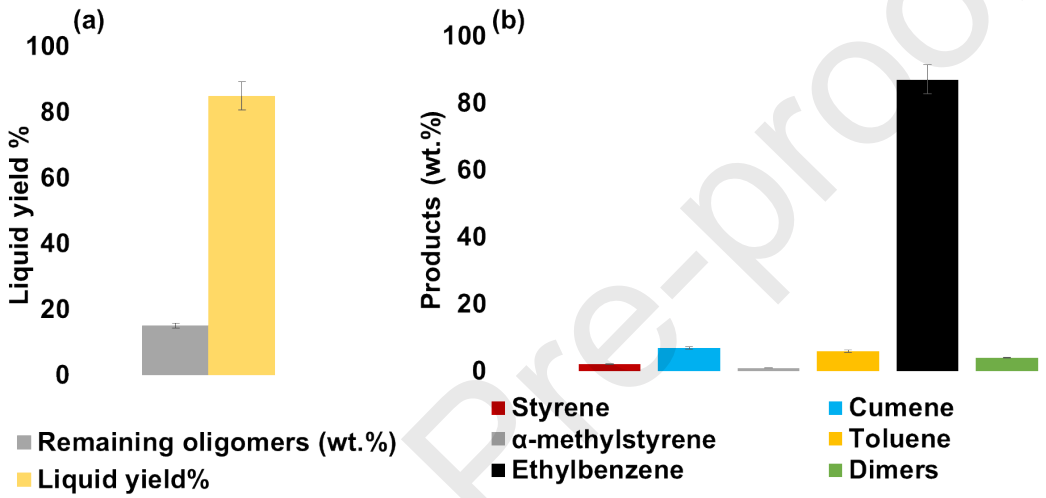

Figure 2 PS degradation over Fe-Cu-Co/Alumina (a) the liquid yield versus the remaining oligomers yields (b) products selectivity (Conditions: reaction temperature 250 °C, exposure time: 90 min., catalyst loading: 0.20 g, PS loading: 2.0 g, and under air).

Table 1 The reported bimetallic catalysts result in the literature (A* in the table stands for Aromatics).

Catalyst	Liquid Y%	Temp. (°C)	Environ.	Liquid	Ref.
Ni-Mo/Al_2O_3	70	375	H_2	A*	[15]
Ni-Mo/Al_2O_3	70.9	400	N_2	A*	[15]
Co-Mo/Al_2O_3	77.3	375	H_2	A*	[15]
Co-Mo/Al_2O_3	72.6	400	N_2	A*	[15]
Fe-Co/SiO_2	80.5	375	H_2	A*	[15]
Fe-Co/SiO_2	71.9	400	N_2	A*	[15]
Ni-Fe-Co/SiO_2	74.7	400	N_2	A*	[15]
Ni-Fe-Co/SiO_2	73.6	375	H_2	A*	[15]
Fe-Cu/Al_2O_3	66	250	N_2	A*	[6]
Fe-Co/Al_2O_3	90	250	N_2	A*	[7]
Fe-Cu-Co/Al_2O_3	**82**	**250**	**Air**	**EB**	**This work**

Table 2 FeCuCo/Alumina catalytic reproducibility and selectivity (T=250 °C, t=90 min., catalyst weight= 200 mg)

Experiment No.	**EB.**	**SM.**	**SD.**	**Cum.**	**Tol.**	**α-MS.**
First	81	4	3	6	5	1
Duplicate	82	4	2	6	5	1
Triplicate	82	3	2	7	5	1

[1]Ethylbenzene (EB.), Styrene monomer (SM.), dimers (SD), Cumene (Cum.), Toluene (Tol.) and α-Methyl styrene (α-MS)

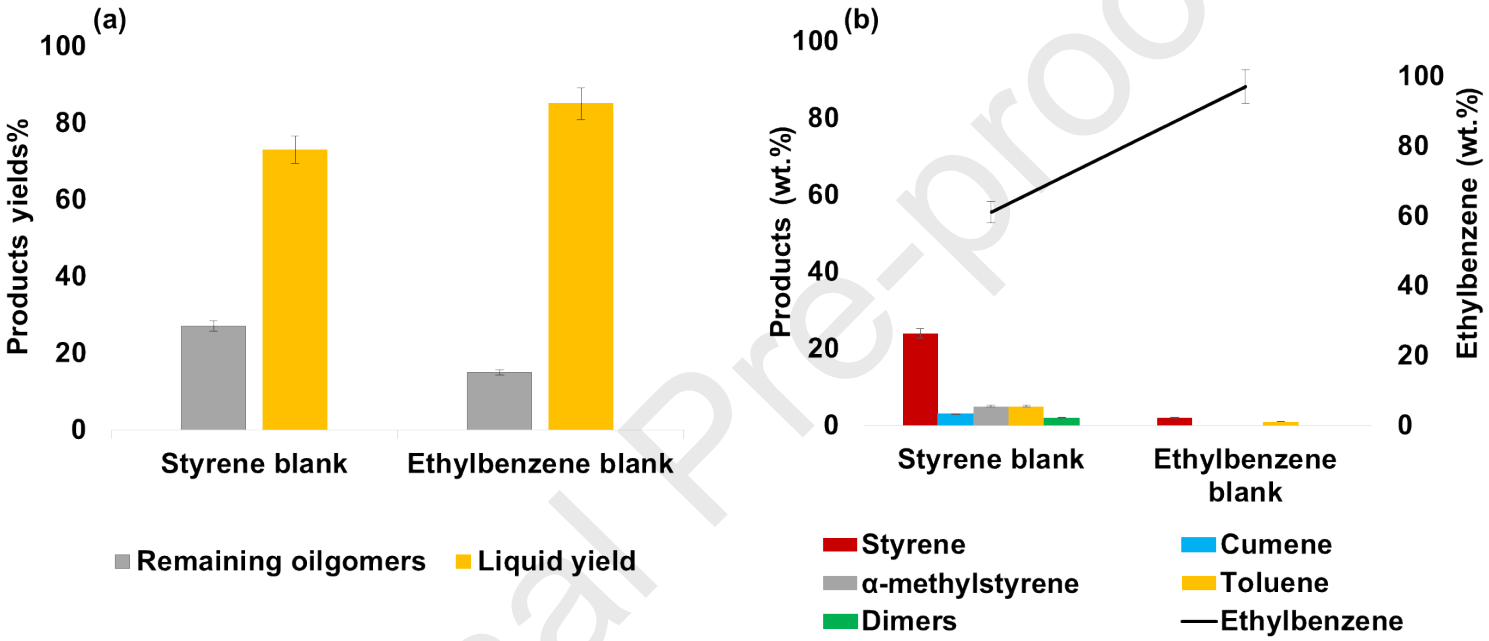

Figure 3 Control experiments of styrene and ethylbenzene reactivity in the presence of Fe-Cu-Co/Alumina (a) product yields and (b) Products selectivity in wt.% (Conditions: reaction temperature 250 °C, catalyst loading: 0.20 g, exposure time: 90 min., and under air).

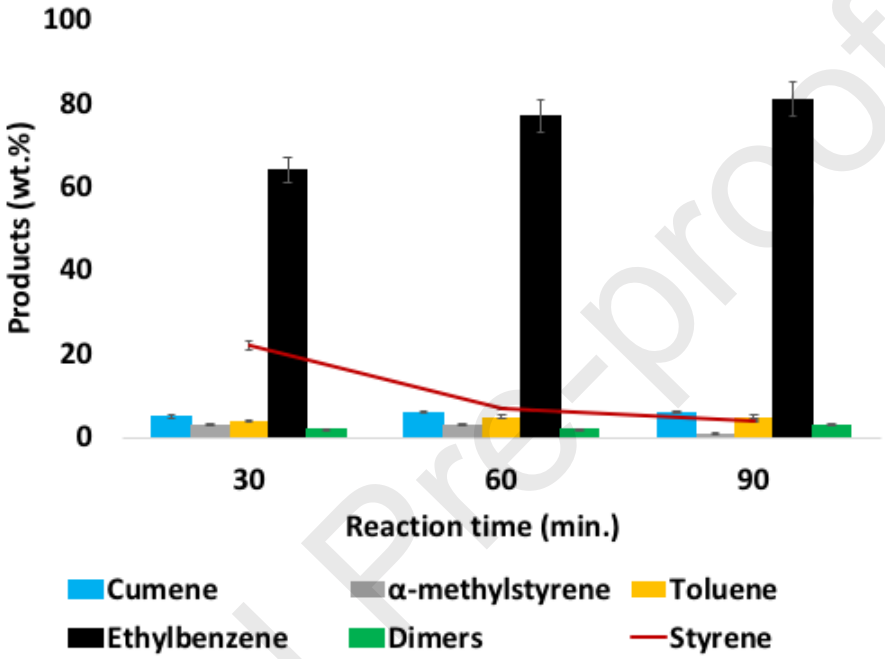

Figure 4 Exposure time effect on the transformation of PS into EB (Conditions: reaction temperature 250 °C, catalyst weight: 0.20 g, PS weight: 2.0 g, and under air).

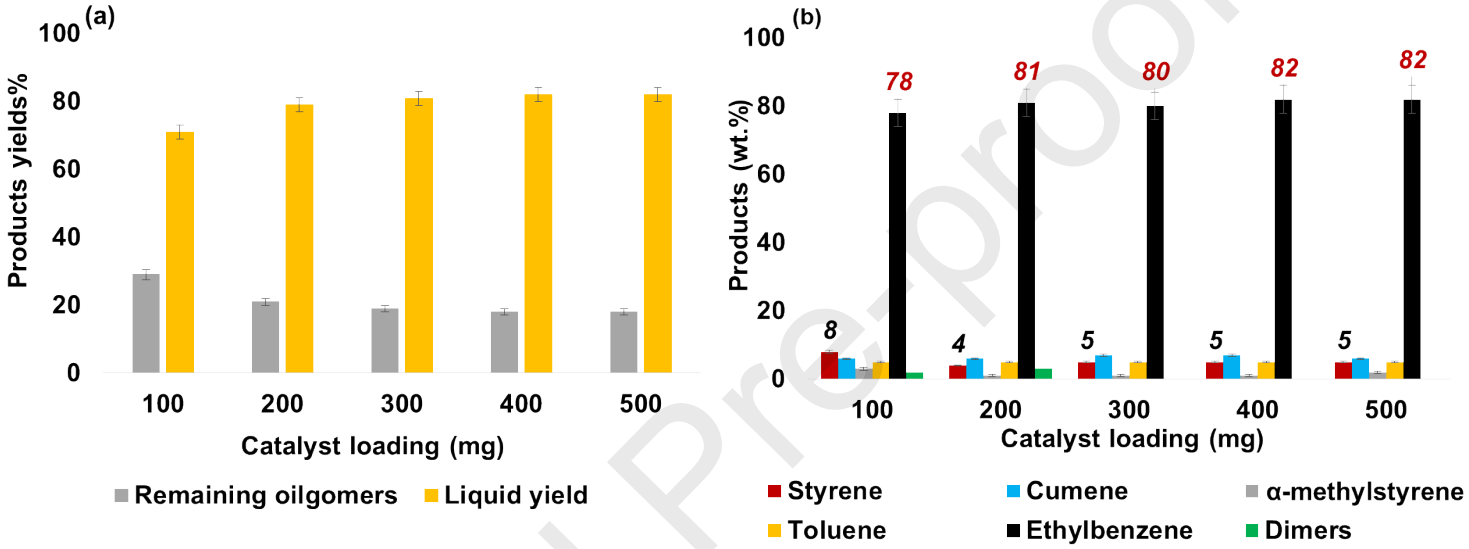

Figure 5 Fe-Co-Cu\Alumina loading effect on the products selectivity (Conditions: reaction temperature 250 °C, exposure time: 90 min., PS loading: 2.0 g, and under air).

Table 3 XPS elemental analysis of fresh & spent FeCuCo/Alumina**.**

Element	**Fresh**	**Spent**
Fe	0.78	0.38
Cu	0.37	0.25
Co	0.47	0.38
Al	38.03	27.85
O	44.99	33.14
C	15.35	37.99